Permanent Magnet-Assisted Omnidirectional Ball Drive

Ayberk Özgür[1], Wafa Johal[1,2] and Pierre Dillenbourg[1]

***Abstract*—We present an omnidirectional ball wheel drive design that utilizes a permanent magnet as the drive roller to generate the contact force. Particularly interesting for novel human-mobile robot interaction scenarios where the users are expected to physically interact with many palm-sized robots, our design combines simplicity, low cost and compactness. We first detail our design and explain its key parameters. Then, we present our implementation and compare it with an omniwheel drive built with identical conditions and similar cost. Finally, we elaborate on the main advantages and drawbacks of our design.**

I. Introduction

In robotic locomotion, specialized scenarios are particularly interesting where one or more aspects of locomotion hardware are highlighted; such examples are affordabilitiy in swarm robotics due to the requirement of many robots; accuracy and repeatability in industrial robotics due to quality requirements; holonomicity in service robotics for maneuverability *etc.* Our focus is a novel human-robot interaction setting that involves many palm-sized mobile robots working simultaneously on a tabletop surface where they not only convey information via their presence and actuation in the classical manner (*i.e.* pose, LEDs, sound *etc.*) but are also intended to be often manipulated by the user as a tangible item and/or to receive haptic feedback: Such robots *can move and be moved*.

One potential application of these robots is a novel interface for interacting with (many) virtual point-like objects that reside on a plane. Here, the robots represent the spatial presence and motion of these objects while responding to the user haptically upon physical interaction (*e.g.* conveying virtual forces that act on the objects); in this sense, the robots act as "autonomous mice". Moreover, multiple robots can autonomously come together to form arbitrary shapes, enhancing the spatial representation and haptic output capabilities. A more concrete application that builds upon these ideas is a novel teaching platform for basic education. Here, the robots represent various objects depending on the activity and subject (*e.g.* particles of matter in chemistry, vertices of a polygon in geometry) where they simulate how the objects behave or act as "haptically active" input/output devices in the given scenario. The goal would be to teach the core material more efficiently by exploiting methods such as kinesthetic learning using the robots' autonomy and haptic feedback capabilities.

This novel setting requires that our mobile robot is small enough to be entirely graspable. When held, it must allow being externally driven and be able to give haptic feedback in any direction; therefore, it must be holonomic. As the required design is intended for consumer devices, it must minimize cost (sacrificing precision if needed) and fit inside a small enough volume using readily available parts so as to minimize custom machining need. We hypothesize that these requirements can be met rather efficiently using a *ball wheel drive* (*i.e.* omnidirectional drive where each wheel is spherical with at least 2 DOF) due to its typical simplicity and compactness.

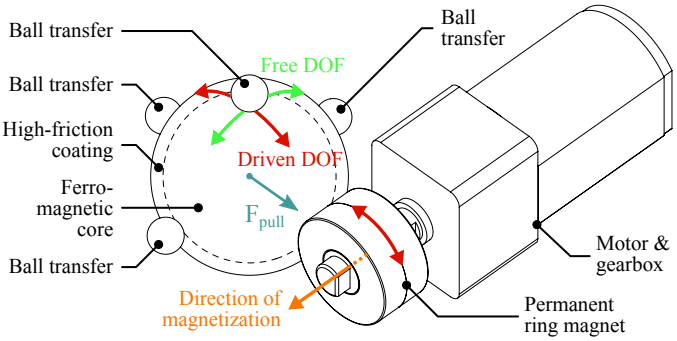

Fig. 1. Overview of our design. The ball wheel with ferromagnetic core is driven by a permanent ring magnet that acts as the drive roller. The magnet temporarily magnetizes the wheel, exerting a pull force and generating the necessary normal force. The wheel thus acquires one driven and one free DOF, kinematically equivalent to an omniwheel.

[1] describes the first two examples of ball drives where the wheel rests against rollers mounted around a tilted ring. [2, 3, 4] describe schemes where the wheel is driven by an omni-wheel in one axis and is free to rotate in the remaining axes. In [5] and [6, Tribolo robot], the wheel is driven by a roller located on its horizontal great circle, allowing it to rotate freely around the horizontal axis orthogonal to the driven axis.

[7] proposes a redundant scheme where each wheel is driven by two orthogonal rollers in a 3-wheel configuration. Each roller's contact forces are actively regulated by pneumatic pistons to reduce wheel coating wear and increase obstacle robustness. [8] also features two drive rollers but with two spring-loaded sensor rollers opposite the drive rollers that encode wheel rotation and help detect drive roller-wheel slip.

[9, 10, 11, 12] describe dynamically stable robots on a single ball wheel driven by (at least 2) omnidirectional/semi-omnidirectional wheels/rollers. [13] proposes a similar design where the single ball wheel is driven by two rollers, but the robot is enclosed in a spherical shell where the center of mass is located lower than the geometric center, ensuring that no dynamic balancing is needed to stay upright.

All above studies use rotating contact elements to drive the wheel, but there are alternative methods. [14] proposes a

[1]Computer-Human Interaction in Learning and Instruction (CHILI)
[2]Laboratoire de Systèmes Robotiques (LSRO)
Ecole Polytechnique Fédérale de Lausanne (EPFL), Switzerland
Email: firstname.lastname@epfl.ch

spherical induction motor scheme where a copper-over-iron spherical shell (acting as rotor) is omnidirectionally driven by multiple curved stators. [15] proposes driving a spherical wheel with an ultrasonic motor; this method has the potential for exceptional compactness and low cost.

In this study, we present a novel ball drive design (seen in Figure 1) that utilizes the force exerted by a permanent magnet to generate the normal force that ensures the friction force driving the ball wheel. Our design is aimed to lower the cost and ease miniaturization (which are concerns mostly absent from past ball drive studies) and we believe that it is simple yet robust enough to be readily used in palm-sized consumer devices for holonomic locomotion. In the following sections, we describe the principles in our design, present our low-cost implementation, quantitatively validate its performance against a baseline and finally assess its strengths and weaknesses.

II. Design

A. Overview & Key Principles

Our ball drive design, seen in Figure 1, has a permanent ring magnet[1] located on the horizontal great circle of the wheel, acting as the drive roller. With the normal force generated by the magnetostatic interaction (*i.e.* pull) between the magnet and the wheel, the magnet can ideally drive the wheel around its axis of rotation thanks to the static contact friction while the wheel remains free to rotate around the orthogonal axis on the horizontal plane.

The placement ensures that the magnetostatic interaction stays isotropic regardless of the wheel's or magnet's orientations, assuming that the wheel's core is magnetically isotropic in all directions and the magnet is magnetically isotropic around its rotation axis. Other important assumptions for isotropy are that the wheel core material is chosen appropriately and the wheel rotates slowly enough so that the parasitic forces due to the magnetic after-effect and induced eddy currents in the wheel are negligible. For example, it was empirically observed that these effects are significantly stronger with an AISI 440C stainless steel core wheel compared to an AISI 1010 carbon steel core wheel.

Utilizing the magnetostatic interaction to ensure the contact conditions eliminates the need for external elements that would normally ensure these conditions such as spring loaded passive rollers. In other words, the contact force mechanism is naturally embedded in the wheel and the drive roller that is the magnet. Given a wheel diameter, the normal force magnitude can be controlled in design by choosing the magnet size (analysis in the next section) and strength.

The ball wheel is loosely enclosed in a space defined by the drive roller and 4 ball transfer units: above the wheel (bears the weight of the robot), opposite the drive roller and finally on the left and right of the wheel. As a design choice, the motor is not fixed on the frame and is left free to move along the plane perpendicular to the driven axis. The drive roller and the wheel are also free to move along this plane but are constrained by the frame and the ball transfers respectively: They are only allowed to move a very small amount such that the disturbance on the system's geometry is minimal. The magnetic pull force ensures that the wheel-drive roller contact remains unbroken during these motions.

[1]An axially magnetized ring magnet (poles on the top & bottom) was preferred over a radially magnetized one (poles on the inside & outside) due to cost and availability.

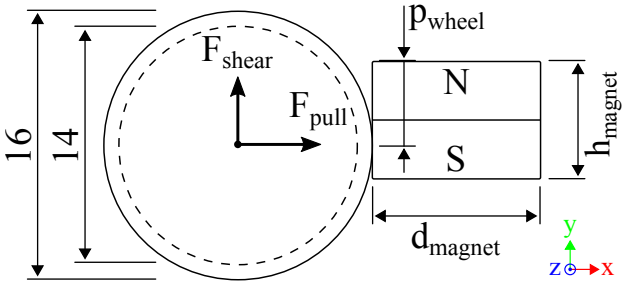

Fig. 2. Magnetostatic wheel-magnet interaction analysis parameters (h_{magnet}, d_{magnet} and p_{wheel}) and calculated quantities (F_{shear} and F_{pull}), top-down view, dimensions in mm. Ring magnet hole diameter was set to 40% of d_{magnet}.

When the robot is externally manipulated, either the ball wheel will rest against the opposite ball transfer (seen in Figure 5a) or the drive roller will rest against the frame (seen in Figure 5b), depending on the actuation and manipulation forces: This redirects all external manipulation loads to ball transfers and/or the frame and prevents them from resulting in shear loads on the motor shaft. Although this method results in reduced precision, increased friction and backlash at the wheel level, it adds robustness against human interaction and potentially increases motor and gearbox lifetime using no extra parts.

A final consideration is the encoding of wheel rotation for odometry, which is not trivial for a design such as ours. Two low-cost solutions in the literature are optical mouse sensors on wheels (such as the one in [14]) and rotary encoders on the motor shaft. Our solution is to use the absolute global localization method described in [16]. This method is based on decoding a printed structured microdot pattern on the ground with an onboard camera; although it is very low cost, it is robust against motion, works in real time and can ensure sub-mm accuracy. With this, we estimate the wheel velocities using the robot velocity (v_x, v_y, ω) with inverse kinematics.

B. Magnetostatic Wheel-Magnet Interaction Analysis

The magnetostatic interaction between the ball wheel and the magnet depends on the physical dimensions of both objects and is not trivial to predict. Given such dimensions, it is desirable to know where the ball will rest along the height of the magnet (if it rests at all) and how much force will be exerted on it. In order to determine these, the pull and shear forces on the wheel were calculated using *COMSOL Multiphysics* (Finite Element Analysis software) for fixed ball wheel dimensions and parametric magnet dimensions and position, as seen in Figure 2. The obtained shear forces were then used to calculate the potential of the wheel in order to determine its resting position. Throughout the section, the wheel resting position (*i.e.* p_{wheel}) is given in percentages of the magnet height (*i.e.* h_{magnet}) to remain invariant to the magnet height parametrization: 0% corresponds to the upper edge, 50% corresponds to midway between two edges *etc.*

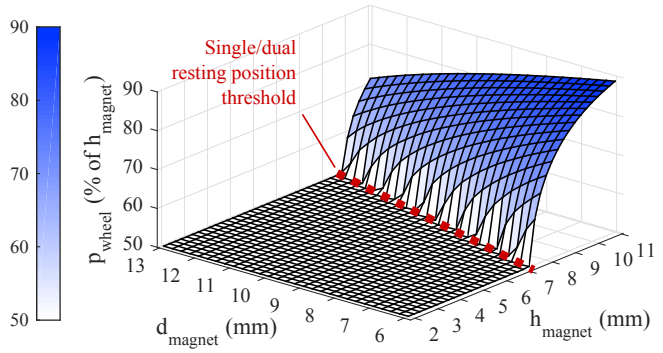

(a) Wheel resting positions. For every $p_{wheel} \neq 50\%$ (above threshold), there is trivially a second resting position at $100\% - p_{wheel}$ (not shown above) due to magnet's symmetry.

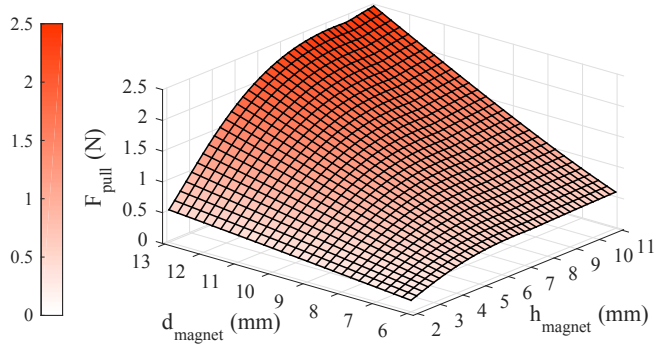

(b) Pull forces exerted on the wheel at resting position(s).

Fig. 3. Magnetostatic wheel-magnet interaction analysis results. Wheel core permeability assumed to be $\mu_r = 500$, magnet magnetization assumed to be $M = 9.75 \times 10^6$ Am^{-1} (calibrated by measuring force on real magnet).

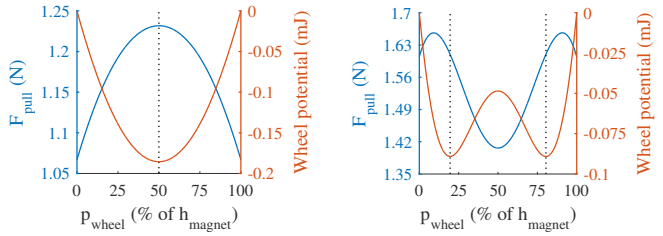

(a) $d_{magnet} = 10$mm, $h_{magnet} = 5$mm

(b) $d_{magnet} = 10$mm, $h_{magnet} = 11$mm

Fig. 4. Pull forces and wheel potentials for selected magnet dimensions. Resting positions are marked with dotted lines.

The results of the analysis, namely resting positions and pull forces, are given in Figures 3a and 3b respectively. Considering the resting positions in the parameter space, it can be seen that there exists a threshold below which the wheel rests at the center of the magnet (example in Figure 4a), requiring small enough h_{magnet} and large enough d_{magnet}. For all such pairs of magnet dimensions, F_{pull} is observed to be symmetric around the resting position. Beyond this threshold, the wheel rests at two symmetric positions which quickly move away from the center towards the edges with larger h_{magnet} and smaller d_{magnet} (example in Figure 4b), but the wheel rests at some position along the magnet height and is not pulled entirely towards the poles (at least not within the tested parameter space). However, for all such pairs of magnet dimensions, F_{pull} is observed to not be symmetric around the resting positions. Finally, it is observed that F_{pull} at resting position(s) increases almost linearly with increasing d_{magnet}, but tends to increase and saturate with increasing h_{magnet}. Therefore, after a point, there is little or no F_{pull} gain with increased h_{magnet}.

Given the analysis results, we chose to remain within the single resting position region; it is desirable to have symmetric F_{pull} magnitude around the resting position, since the wheel will inevitably move a small amount along the magnet height due to inaccuracies during motions involving its free DOF in a multi-wheel configuration. In this region, the smallest geometrically feasible pair of off-the-shelf dimensions that would ensure enough F_{pull} was chosen, which corresponds to $d_{magnet} = 10$mm and $h_{magnet} = 5$mm.

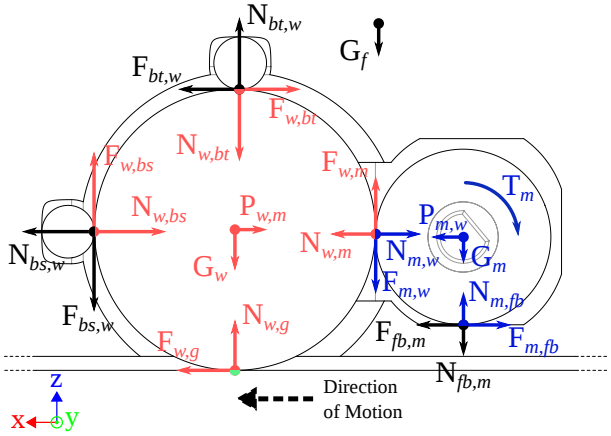

(a) Forward mode.

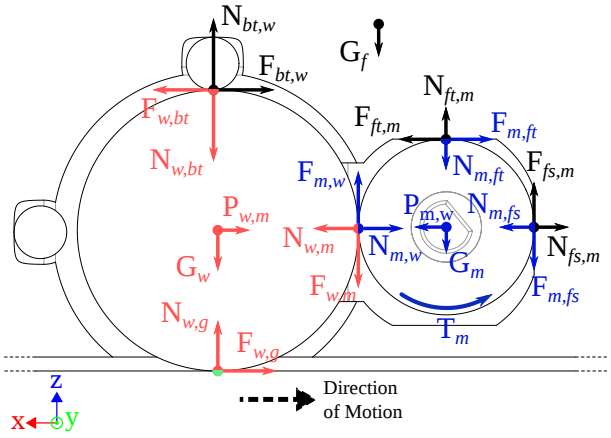

(b) Backward mode.

Fig. 5. Dynamics of ball drive, side view. Normal, friction, gravity and magnetic pull forces denoted with N, F, G and P respectively. Torque denoted with T. Ball wheel, magnet, frame and ground (rigid bodies) denoted with *w*, *m*, *f* and *g* respectively. Different contact points on frame denoted with *bs*, *bt* (ball transfers), *ft*, *fs* and *fb* (surfaces acting as plain bearings). Forces acting on wheel, magnet and frame colored in *red*, *blue* and *black* respectively.

C. Dynamics of Single Ball Drive

The nature of our design implies highly unideal conditions with sources of additional friction (low-performance ball transfer units, magnet resting against frame surfaces instead of being supported by the motor shaft) which requires careful analysis of the dynamics of our system, as seen in Figure 5

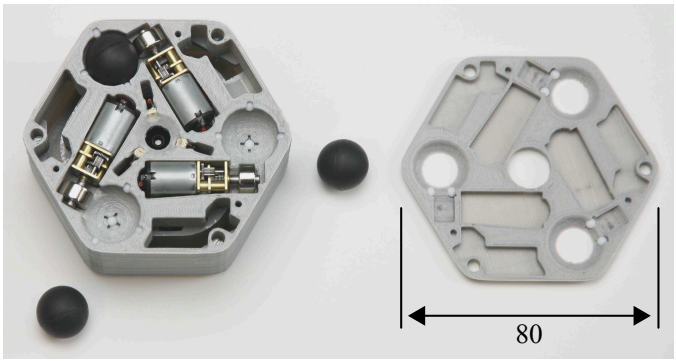

Fig. 6. Ball drive implementation, size given in mm. Main body (on the left) rests bottom-side-up. Bottom "lid" opened (on the right) and two ball wheels removed from enclosures for better visibility of internals. In the center, camera lens aperture and 3 exposure LEDs used for localization are seen.

for a single ball drive. When the force exerted on the ground ($F_{w,g}$, in N) is calculated in terms of the applied motor torque (T_m, in Nm) given practical materials[2] and weights, it is seen that the dynamics of the system differ significantly depending on the motor torque (derivation omitted):

$$F_{w,g} = \begin{cases} 140.0T_m - 0.0648 & \text{if } \textit{forward} \text{ and } T_m < 0.00180 \\ 128.0T_m - 0.0441 & \text{if } \textit{forward} \text{ and } T_m > 0.00180 \\ 126.0T_m - 0.0108 & \text{if } \textit{backward} \end{cases}$$

In *forward mode*, with small enough torque (first case above), the system enters a degenerate state where the robot frame is only accelerated by the top ball transfer and magnet-frame contacts (*i.e.* by $F_{fb,m} + F_{bt,w}$ where $N_{bs,w} = 0$ and $N_{fs,m} \neq 0$). In all cases, wheel-ground slip always occurs before wheel-magnet slip thanks to the magnetic pull force (*backward mode* torques indicated with negative values):

$$T_m = \begin{cases} 0.00531 & \Longrightarrow \text{ wheel-magnet slips} \\ 0.00442 & \Longrightarrow \text{ wheel-ground slips} \\ -0.00424 & \Longrightarrow \text{ wheel-ground slips} \\ -0.0596 & \Longrightarrow \text{ wheel-magnet slips} \end{cases}$$

This analysis covers the dynamics of each wheel independently under assumptions such as the existence of 3 wheels in total and equal weight distribution per wheel. However, the dynamics of a given wheel depends also on the dynamics of other wheels and the overall geometry of the system. Moreover, external manipulation by users may affect the dynamics, and may require additional sensors to detect and handle correctly. These concerns are not considered in this study and will be addressed in the future.

III. Implementation

The proposed ball drive was implemented in the widely used 3-wheel configuration (same kinematics as [2, 3, 5]), as seen in Figure 6. In such scales, the natural placement of the motor on the side of the ball wheel allows a compact arrangement of the components (also mentioned by [5]). The frame (including ball transfer enclosures embedded within it) and motor shaft adapters for the magnets were manufactured using Fused Filament Fabrication (FFF) with Polylactic Acid (PLA). The frame has a hexagonal form (73mm width, 80mm end-to-end) enclosing all locomotion components and isolating them from the exterior except three 11mm-diameter holes on the bottom where the wheels are exposed. The ground clearance is 0.8mm and the entire locomotion subsystem fits inside a height of 19mm, measured from the ground.

Apart from the above, all components are off-the-shelf. This includes the ball transfer units which are simple Polytetrafluoroethylene (PTFE) balls enclosed in the frame. Two more were added to the bottom of each wheel to keep them from contacting the frame when the robot is picked up; they are not active during normal motion. The wheels are AISI 1010 carbon steel balls with a 1mm-thick Nitrile Butadiene Rubber (NBR) coating of Shore A 90 hardness. These and other components are listed in Table I with their typical cost.

TABLE I
List of off-the-shelf components and their cost

Component (off-the-shelf)	**Cost (€)**
Ball wheels (14mm AISI 1010 core, 1mm NBR coating)	1.30×3
Ball transfer units (3mm PTFE)	0.06×18
Magnets (Neodymium, N42 magnetization, Ni plating)	0.44×3
Motors (Pololu micro metal-gear motor, 30:1, MP)	13.18×3
Motor drivers (BD6210HRP)	1.31×3
Localization subsystem ([16], includes processor)	25.75
Total	**75.52**

The motors are driven with a motion controller that tracks a command pose by determining the required robot velocity (v_x, v_y, ω) in a closed loop fashion (PID). Wheel velocities (v_1, v_2, v_3) are then calculated from the required robot velocity (using inverse kinematics and the current global orientation of the robot) and are set in a calibrated open loop that takes the results of the analysis in Section II-C into account. This simple controller was observed to be adequate for the evaluation made in the following section, and will be improved in the future.

IV. Comparative Evaluation

A. Experiment Design

In order to test the performance of our design against a baseline, we built an alternative version of our robot with omniwheels (as it is one of the most prevalent methods of omnidirectional motion), seen in Figure 7, with the same geometry and kinematics except the wheel offset from center (28mm *vs.* 46.9mm). The same manufacturing methods and components were used except 50:1 gear reduction motors instead of 30:1. Care was taken during frame manufacturing that both robots have roughly the same weight (178.9g *vs.* 178.1g). The 30mm-diameter omniwheels were custom manufactured due to the lack of such a small size off-the-shelf: The rims were manufactured with FFF while the rollers

[2]Using components described in Section III: $P_{m,w} = 1.232$N, $\mu_k^{\text{magnet-frame}} = 0.37$ (measured), $\mu_k^{\text{wheel-ball transfer}} = 0.07$ ([17]), $\mu_s^{\text{magnet-wheel}} = 0.82$ (measured), $\mu_s^{\text{wheel-ground}} = 0.8$ (assumed, depends on ground material)

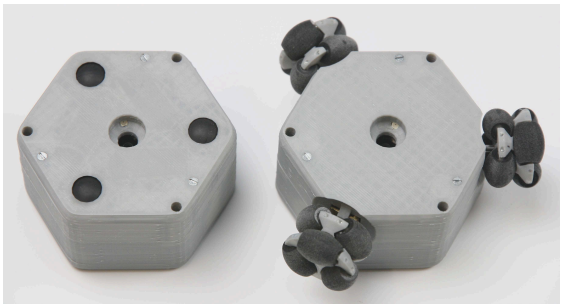

Fig. 7. Omniwheel drive robot built as a baseline, in comparison with ball drive robot. Both robots rest bottom-side-up.

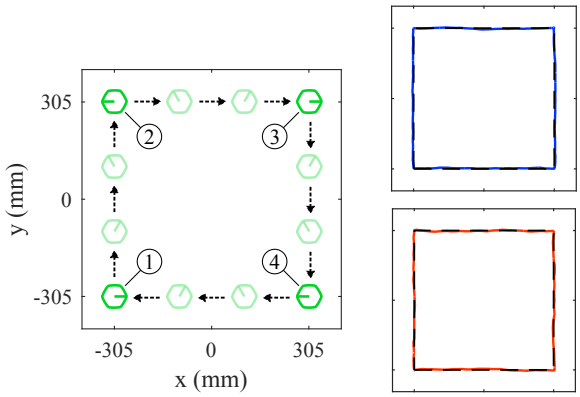

Fig. 8. Trajectory for performance evaluation (left); robots were simply commanded to move to the next goal pose with given maximum velocities at poses ①, ②, ③ and ④. Typical x, y trajectories executed by ball drive robot (top right, blue) and by omniwheel drive robot (bottom right, red).

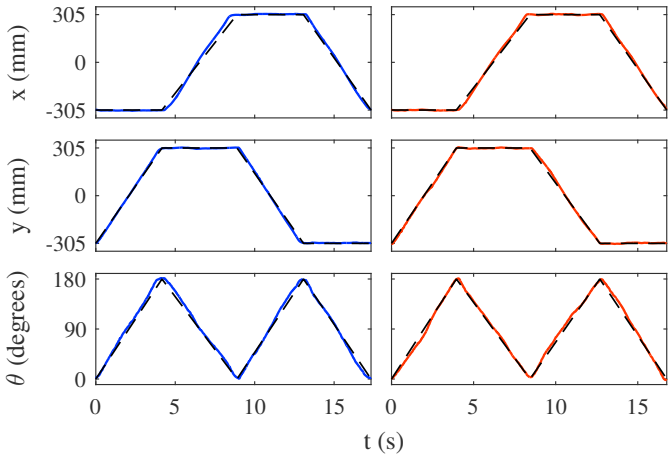

Fig. 9. Typical trajectories followed by robots. Left column (in blue): Ball drive robot. Right column (in red): Omniwheel drive robot. Dashed lines indicate values of ideal trajectory.

TABLE II
COMPARATIVE PERFORMANCES OF PROPOSED AND BASELINE DRIVES
(VALUES GIVEN WITH ± ONE STANDARD DEVIATION)

Mode	Measured quantity	Ball drive	O.w. drive
Mean	$\lvert x_{\text{sampled}} - x_{\text{ideal}} \rvert$ (mm)	11.1 ± 11.3	7.53 ± 8.26
	$\lvert y_{\text{sampled}} - y_{\text{ideal}} \rvert$ (mm)	6.52 ± 7.07	6.66 ± 7.80
	$\lvert \theta_{\text{sampled}} - \theta_{\text{ideal}} \rvert$ (deg)	5.40 ± 3.80	4.40 ± 3.14
Worst	$\max \lvert x_{\text{sampled}} - x_{\text{ideal}} \rvert$ (mm)	44.6 ± 4.48	33.3 ± 6.31
	$\max \lvert y_{\text{sampled}} - y_{\text{ideal}} \rvert$ (mm)	30.8 ± 7.44	34.0 ± 4.84
	$\max \lvert \theta_{\text{sampled}} - \theta_{\text{ideal}} \rvert$ (deg)	14.9 ± 2.00	12.9 ± 1.94

(hard plastic core, 1mm-thick Shore A 85 hardness rubber-like exterior) were manufactured with Multi Jet Modeling (MJM) for 2.18€ per roller. The same motion controller was used with appropriately calibrated coefficients in both robots.

Both robots were commanded to follow the square trajectory seen in Figure 8 with 150mm/s maximum linear velocity and $\pi/4.067$ rad/s maximum angular velocity (ball drive robot run can be viewed in the video attachment). These commands were given on the corners of the trajectory when they are reached, *i.e.* a total of 4 times. The particular usage of global localization in the motion controller ensures that the goals are eventually reached, but the controller does not ensure tracking of real velocities and therefore fidelity to the ideal trajectory in a closed loop. 10 runs were done for each robot where pose data were collected at about 46.6Hz from the robot's own global localization system. In this setup, the sources of significant systematic error are identified as:

- FFF and MJM tolerances, notably for magnet-shaft adapters, ball transfer housings and omniwheel rollers
- Ball wheel fabrication tolerances: Off-center core results in anisotropic moment of inertia and magnetic forces
- Off-the-shelf motor variances, causing some wheels to consistently rotate more than others with the same input

B. Results & Discussion

To compare the performances of the two robots, deviations from the ideal trajectory (defined as the accelerationless constant-velocity trajectory from one command pose to the next) were calculated for each sample, separately for x, y and θ. Typical motions of the robots can be seen in Figure 9 while the overall performances are compared in Table II; in **mean**, all samples from all 10 runs were taken ($N_{\text{ball drive}} = 8183$, $N_{\text{o.w. drive}} = 7705$) while in **worst**, maximum deviation of each run was taken ($N_{\text{ball drive}} = N_{\text{o.w. drive}} = 10$).

The results indicate that the omniwheel drive performed better in x and θ while the difference in y was not statistically discernible. However, when the mean deviations are compared with the trajectory lengths, it is seen that the deviations differ by 0.31%, 0.01% and 0.14% of the total trajectory length for x, y and θ respectively. When the worst deviations from each of the 10 runs are considered, the deviations differ by 0.93%, 0.26% and 0.28% of the total trajectory length.

Additionally, the omniwheel drive was visually observed to vibrate significantly more compared to the ball drive due to discontinuous contact points with the ground, as predicted by the literature (*e.g.* [2, 3, 7, 8]). As mentioned previously, the proposed ball drive design also tends to be more geometrically compact (both horizontally and vertically) compared to a kinematically equivalent omniwheel drive design. If the performance differences provided above (and other shortcomings) can be tolerated in a given application, the ball drive design can be preferred over the traditional omniwheels for these (and other) added benefits.

V. Conclusions

In this study we presented a novel element for ball drives, namely permanent magnet support, that will potentially lower cost and increase miniaturizability. Our design,

- Is almost fully made of low cost off-the-shelf components
- Has naturally compact geometry that enables it to fit inside a palm-sized robot with such components
- Produces less vibrations and has smoother motion compared to omniwheels
- Has smaller and simpler mechanical components that must be exposed to the outside world compared to omniwheels (rubber sphere segments *vs.* omniwheel rim ends and rollers), potentially reducing distractions and cognitive load in (mainly younger) users
- Has equivalent control on drive roller-wheel contact force with simpler elements, compared to traditional passive mechanisms in other ball drive designs (*e.g.* spring-loaded passive roller, drive roller deformation)
- Is robust against physical user interaction by virtue of magnetic force preservation which permits leaving the magnet-wheel assembly unmounted from the frame

However, it also comes with certain drawbacks. Our design,

- Is not suitable for high-precision applications
- Requires robot to be lightweight enough due to low load bearing capabilities of simple ball transfer units
- Requires robot to be small enough in size; larger robots would require potentially too large and dangerous magnets and too heavy ball wheels
- Requires flat enough surface (*e.g.* tabletop) to run on due to low ground clearance
- Requires encoding ball wheels which is not trivial
- Has less simple dynamics compared to omniwheels
- Produces more audible noise compared to omniwheels due to the frame acting as plain bearing for the magnet
- May require maintenance in long-term use due to extensive use of contact dynamics and potentially due to accumulation of foreign materials in the bearings

We believe that our omnidirectional drive design, being affordable but still robust against human manipulation, is particularly useful for human-robot interaction settings where many small mobile robots capable of haptic interaction on some level must be present. In the future, dynamics of our drive will be studied as a complete system in the presence of user manipulation in order to develop a motion/haptic feedback controller, with additional sensors if necessary. Finally, focused user studies will be done to evaluate further qualities of our design such as user friendliness and haptic fidelity.

Acknowledgements

We would like to thank the Swiss National Science Foundation for supporting this project through the National Centre of Competence in Research Robotics and Dr. Michel Lauria for participating in the design of the Tribolo robot which inspired us to pursue a ball drive design.

References

[1] M. West and H. Asada. Design of Ball Wheel Mechanisms for Omnidirectional Vehicles with Full Mobility and Invariant Kinematics. *J. of Mech. Design*, 119(2): 153–161, 1997.

[2] L. Ferrière and B. Raucent. ROLLMOBS, a new universal wheel concept. In *Int. Conf. on Robotics and Automation*, pp. 1877–1882 vol.3, 1998.

[3] H. Ghariblu et al. Design and Prototyping of Autonomous Ball Wheel Mobile Robots. In *Mobile Robots - Current Trends*. InTech Open Access Publisher, 2011.

[4] B. Gebre et al. A Multi-Ball Drive for Omni-Directional Mobility. In *Int. Conf. on Technologies for Practical Robot Applicat.*, pp. 1–6, 2014.

[5] D. Ball et al. A Practical Implementation of a Continuous Isotropic Spherical Omnidirectional Drive. In *Int. Conf. on Robotics and Automation*, pp. 3775–3780, 2010.

[6] R. Siegwart et al. *Introduction to Autonomous Mobile Robots*. MIT Press, 2011.

[7] Y. Lee et al. Control of a redundant, reconfigurable ball wheel drive mechanism for an omnidirectional mobile platform. *Robotica*, 25(04):385–395, 2007.

[8] G. Runge et al. Design and Testing of a 2-DOF Ball Drive. *J. of Intelligent & Robotic Syst.*, 81(2):195–213, 2016.

[9] T. Endo and Y. Nakamura. An Omnidirectional Vehicle on a Basketball. In *Int. Conf. on Advanced Robotics*, pp. 573–578, 2005.

[10] T. B. Lauwers et al. A Dynamically Stable Single-Wheeled Mobile Robot with Inverse Mouse-Ball Drive. In *Int. Conf. on Robotics and Automation*, pp. 2884–2889, 2006.

[11] M. Kumagai and T. Ochiai. Development of a Robot Balancing on a Ball. In *Int. Conf. on Control, Automation and Syst.*, pp. 433–438, 2008.

[12] M. Kumagai. Development of a Ball Drive Unit using Partially Sliding Rollers -An alternative mechanism for semi-omnidirectional motion-. In *Int. Conf. on Intelligent Robots and Syst.*, pp. 3352–3357, 2010.

[13] W. Chen et al. Design and implementation of a ball-driven omnidirectional spherical robot. *Mechanism and Machine Theory*, 68:35–48, 2013.

[14] M. Kumagai and R. Hollis. Development and Control of a Three DOF Spherical Induction Motor. In *Int. Conf. on Robotics and Automation*, pp. 1528–1533, 2013.

[15] H. Jang et al. Design and Analysis of Ultrasonic Motor for Driving Sphere Wheel. *Ferroelectrics*, 459(1):68–75, 2014.

[16] L. Hostettler et al. Real-Time High-Accuracy 2D Localization with Structured Patterns. In *Int. Conf. on Robotics and Automation*, pp. 4536–4543, 2016.

[17] C. Pooley and D. Tabor. Friction and Molecular Structure: The Behaviour of Some Thermoplastics. *Proc. of the Roy. Soc. of London A: Math., Physical and Eng. Sci.*, 329(1578):251–274, 1972.